International Conference on Space Optics—ICSO 2018

Chania, Greece

9–12 October 2018

Edited by Zoran Sodnik, Nikos Karafolas, and Bruno Cugny

Introducing the atmospheric thermodynamics lidar in Space: ATLAS

Paolo Di Girolamo

Andreas Behrendt

Volker Wulfmeyer

Adolfo Comerón

et al.

International Conference on Space Optics — ICSO 2018, edited by Zoran Sodnik, Nikos Karafolas, Bruno Cugny, Proc. of SPIE Vol. 11180, 111806P · © 2018 ESA and CNES · CCC code: 0277-786X/18/$18 · doi: 10.1117/12.2536160

Introducing the Atmospheric Thermodynamics LidAr in Space – ATLAS

Paolo Di Girolamo*[a], Andreas Behrendt[b], Volker Wulfmeyer[b], Adolfo Comerón[c], Philippe Keckhut[d], Alain Hauchecorne[d], Evelyne Richard[e], Franco Marenco[f], Geraint Vaughan[g], Mathias Rotach[h], Roland Potthast[i], Alan Geer[l], Belay B. Demoz[m], Joseph Santanello[n], David N. Whiteman[n], David D. Turner[o]

[a] Scuola di Ingegneria, Univ. della Basilicata, viale dell'Ateneo Lucano 10, 85100, Potenza, Italy;
[b] Institut für Physik und Meteorologie, Univ. Hohenheim, Garbenstr. 30, 70599 Stuttgart, Germany;
[c] Dept. TSC, Universitat Politècnica de Catalunya, Jordi Girona 1-3, 08034 Barcelona, Spain;
[d] LATMOS- CNRS, 4 place Jussieu, 75252 Paris, France;
[e] Lab. d'Aérologie, Univ. de Toulouse-CNRS, 14 avenue Belin, 31400 Toulouse, France;
[f] Met Office, Fitz Roy Road, Exeter, EX1 3PB, United Kingdom;
[g] University of Manchester, Manchester, United Kingdom;
[h] Depart. of Atmos. and Cryos. Sciences, Univ. of Innsbruck, Innrain 52f, 6020 Innsbruck, Austria;
[i] German Meteorological Service, Offenbach, Germany;
[l] ECMWF, Reading, United Kingdom;
[m] University of Maryland Baltimore County-JCET, Baltimore, MD, U.S.A.;
[n] GSFC - NASA, Greenbelt, MD, U.S.A.;
[o] NOAA / ESRL / GSD, Boulder, CO, U.S.A.

ABSTRACT

Our understanding of the distribution of heat and water in the atmosphere still shows critical gaps on all temporal and spatial scales. This is mainly due to a lack of accurate measurements of water vapor and temperature profiles - hereafter called thermodynamic (TD) profiles - with high vertical and temporal resolution, especially in the lower troposphere. Accurate, high temporal-spatial resolution observations of TD profiles are essential for improving weather forecasting and re-analyses, for studying land-atmosphere feedback processes and for improving model parameterizations of land-surface and turbulent transport processes in the Atmospheric Boundary Layer. These observational gaps can be addressed with a new active remote sensing system in space based on the Raman lidar technique. Combining vibrational and rotational Raman backscatter signals, simultaneous measurements of water vapour and temperature profiles and a variety of derived variables are possible with unprecedented vertical and horizontal resolution, especially in the lower troposphere. This is the key concept of ATLAS, which was submitted in March 2018 to the European Space Agency in response to the Call for Earth Explorer-10 Mission Ideas in the frame of ESA EOEP. An assessment of the expected performance of the system and the specifications of the different lidar sub-systems has been performed based on the application of an analytical simulation model for space-borne Raman lidar systems. Results from the simulations and technical aspects of the proposed mission will be illustrated at the conference.

Keywords: Raman lidar, water vapour, temperature, aerosol, active remote sensing

INTRODUCTION

An appropriate understanding and prediction of Earth's energy and water cycles is fundamental for a sustainable development of the Earth system. However, our understanding of the distribution of heat and water in the atmosphere still shows critical gaps on all temporal and spatial scales [1-3], which is mainly due to a lack of accurate measurements of TD profiles with high vertical and temporal resolution, especially in the lower troposphere [4]. Accurate, high temporal and spatial resolution observations of TD profiles in the lower troposphere from the surface to the interfacial layer at the top of the atmospheric boundary layer (ABL) are essential for improving weather forecasting [e.g., [5], [6]]

and re-analyses [[7]], and understanding the Earth system. Furthermore, these measurements are of primary importance to improve parameterizations of land-surface and turbulent transport processes in the ABL, conducting to a substantial improvement of the representation of clouds and precipitation and the prediction of extreme events,. This is essential for advanced climate projections [[8], [9]]. More specifically, global scale measurements of 3-dimensional TD profiles would have a dramatic impact on our system understanding in four key research areas [[10]]:

i) radiative transfer, as well as regional and global water and energy budgets,
ii) land-atmosphere feedback including the surface energy balance in dependence of soil properties and land cover,
iii) mesoscale circulations and convection initiation [11], and
iv) data assimilation.

Progress in these areas would not only contribute to weather and climate research and forecasting, but also to other related disciplines such as soil, hydrological, and agricultural sciences, in addition to human health and air quality applications.

Observational requirements to be fulfilled by networks of satellite and ground-based remote sensors, with a specific focus on the lower troposphere, have been identified considering four primary application fields: (1) monitoring, (2) verification and calibration, (3) data assimilation and (4) process studies [[10]]. For assessing climate trends, high quality water vapour and temperature measurements are required not only at the Earth's surface, but also throughout the troposphere and stratosphere. This is only partly addressed by the current passive observing systems, as in fact, because of the intrinsic limitations in the inversion of the radiative transfer equation, these systems cannot provide the quality data required to progress in the above areas. This is primarily due to the lack in vertical resolution (>1km), which is insufficient to retrieve vertical gradients in water vapour and temperature profiles, temperature inversions, entrainment processes, etc., especially in the lower troposphere over land, where surface effects strongly limit infrared sounding approaches.

Observational requirements for lower tropospheric water vapour and temperature profiling impose a vertical resolution of ~100 m (i.e. sufficiently high to allow resolving the temperature and moisture gradients), with the bias affecting water vapour mixing ratio and temperature measurements in each single vertical range bin not exceeding 5 % and 0.5 K, respectively, and the random uncertainty not exceeding 10 % and 1 K, respectively. Similar requirements were identified within the World Meteorological Organization Integrated Global Observing Systems [12-14], the World Climate Research Program (WCRP) and the Global Climate Observing System (GCOS) [15]. These observational requirements cannot be met by passive remote sensing techniques (neither in the infrared nor in the microwave region) and can only be fulfilled by a new active remote sensing system in space based on the lidar technique [16,17]. Combining vibrational and rotational Raman backscatter signals, simultaneous measurements of water vapour and temperature profiles and a variety of derived variables are possible with unprecedented vertical and horizontal resolution (see more details in the next section), especially from the surface to the lower troposphere, this being the key concept of the mission Atmospheric Thermodynamics LidAr in Space – ATLAS. The instrument is based on the experience and know-how gained with the development and operation of several existing ground-based instruments [18-31] and airborne instruments [[32]2-34]. On-going and planned lidar missions, such as CALIPSO, CATS, ADM-Aeolus, EarthCARE, have demonstrated the applicability of laser-based active remote sensing in space. ATLAS would complement these missions, being the first space mission based on the Raman lidar technology. Additionally, the impact of ATLAS on weather and climate research can be further enhanced by exploiting synergies with passive instruments on other space platforms, such as IASI-A/B, CrIS and AIRS [35-37] and GNSS occultation.

2. MISSION CONCEPT

The core element of the proposed Earth Explorer mission is a nadir-viewing water vapour and temperature Raman lidar system. In the present mission concept, the Raman lidar is conceived and designed to collect four primary lidar signals: the water vapour vibrational Raman signal, $P_{H_2O}(z)$, the high- and low-quantum number O_2-N_2 rotational Raman signals, $P_{loJ}(z)$ and $P_{HiJ}(z)$, and the elastic backscatter signal at the laser wavelength λ_0, $P_{\lambda_0}(z)$. The direct calculation of atmospheric temperature is obtained from the rotational Raman backscattered signals through the expression [19]:

$$T(z) = \frac{a}{\ln[\frac{P_{HiJ}(z)}{P_{LoJ}(z)}] - b} \quad (1)$$

where, more specifically, $P_{LoJ}(z)$ and $P_{HiJ}(z)$ are the low (*LoJ*) and high (*HiJ*) quantum number rotational Raman backscatter signals in the anti-Stokes branch at wavelengths λ_{LoJ} and λ_{HiJ}, respectively, received from the scattering volume at altitude *z*, and *a* and *b* are two calibration constants. The direct calculation of the water vapour mixing ratio is obtained from Raman backscattered signals through the following equation [38]:

$$x_{H_2O}(z) = K \cdot \Delta Trs(z) \cdot \frac{P_{H_2O}(z)}{P_{ref}(z)} \tag{2}$$

where $P_{H_2O}(z)$ is the water vapour vibrational Raman lidar signal at at wavelength λ_{H_2O}, while $P_{ref}(z)$ is a temperature-independent reference signal obtained from a linear combination of the two temperature sensitive rotational Raman lidar signals $P_{LoJ}(z)$ and $P_{HiJ}(z)$, *K* is a calibration constant [38], *ΔTrs(z)* is a differential transmission term, which accounts for the different atmospheric transmission by molecules and aerosols at λ_{H_2O} and $\lambda_{LoJ\,/\,HiJ}$.

In addition to the temperature and water vapour mixing ratio profile, among the independently measured further products: the particle backscatter and extinction coefficient profiles in the ultraviolet, allowing the determination of the optical properties of aerosol layers and the geometric and optical properties of clouds, thus complementing similar measurements performed with EarthCARE; the profile of relative humidity, the real daytime PBL depth over land and the oceans directly obtained from the temperature profile, as well as atmospheric stability parameters like buoyancy, convective available potential energy (CAPE) and convective inhibition (CIN).

Recent advances in solid-state laser, large-aperture telescope, and detector technologies allow achieving a new performance level from space with the Raman technique. With a laser power of up to 250 W in the ultraviolet and a telescope with a 4 m primary mirror, the above specified observational requirements are reached, thus realizing a breakthrough in earth system sciences. Different candidates for the laser transmitter of ATLAS are available, one of them being a frequency-tripled, diode-laser pumped Nd:YAG laser and another being a frequency-doubled alexandrite laser. The use of a new generation of pump chambers and diode lasers results in a wall-plug efficiency of > 5 %. The receiver will consist of a large-aperture telescope with a diameter of 4 m. Such a telescope would be larger than those in previous lidar missions, but stability and optical quality demands are significantly relaxed (no astronomic quality required) and the receiver technology is comparatively simple and very rugged. Simulations indicate an overall electrical power consumption for ATLAS of ~ 6000 W (5000 W for the laser and 1000 W for the remaining sub-systems). The rough estimate for ATLAS' weight is ~ 600 kg (~ 350 kg for the telescope and ~ 250 kg for the other sub-systems).

An assessment of the specifications of the different lidar sub-systems has been performed with an analytical simulation model for space-borne Raman lidar systems developed at Università della Basilicata [16, 17]. The expected performance was simulated under a variety of environmental and climate scenarios using different atmospheric reference models, which cover various climatic regions and seasons, as well as a variety of solar illumination conditions. In our present simulations the payload is hosted on a frozen dusk/dawn low-Earth sun-synchronous orbit at an altitude of 450 km (inclination ~97 degrees). The horizontal spatial coverage domain is global, i.e. from tropical to sub-polar regions. With daily overpasses at 6/18 h local time, it is possible to capture the TD states before and after the daytime development of the PBL, which are very important for data assimilation in weather forecast models. Figure 1 illustrates the vertical profiles of measurement uncertainty for water-vapour mixing ratio, $\Delta x_{H_2O}(z)/x_{H_2O}(z)$, and of temperature, ΔT, considering the tropical and mid-latitude summer atmospheric models. Considering a vertical resolution of 200 m, values of $\Delta x_{H_2O}(z)/x_{H_2O}(z)$ for the tropical atmosphere are in the range 2-20 % and 3-30 % up to 5.5 km for a horizontal resolution of 50 and 20 km, respectively, while for the mid-latitude summer atmosphere values of $\Delta x_{H_2O}(z)/x_{H_2O}(z)$ are in the range 2-20 % and 3-30 % up to 4 km for a horizontal resolution of 50 and 20 km, respectively. For both the tropical and mid-latitude summer atmosphere values of ΔT are in the range 0.4-1 K and 0.7-1.2 K up to 18 km for a horizontal resolution of 50 and 20 km, respectively. More results from the simulations and more aspects of the proposed mission will be illustrated at the conference.

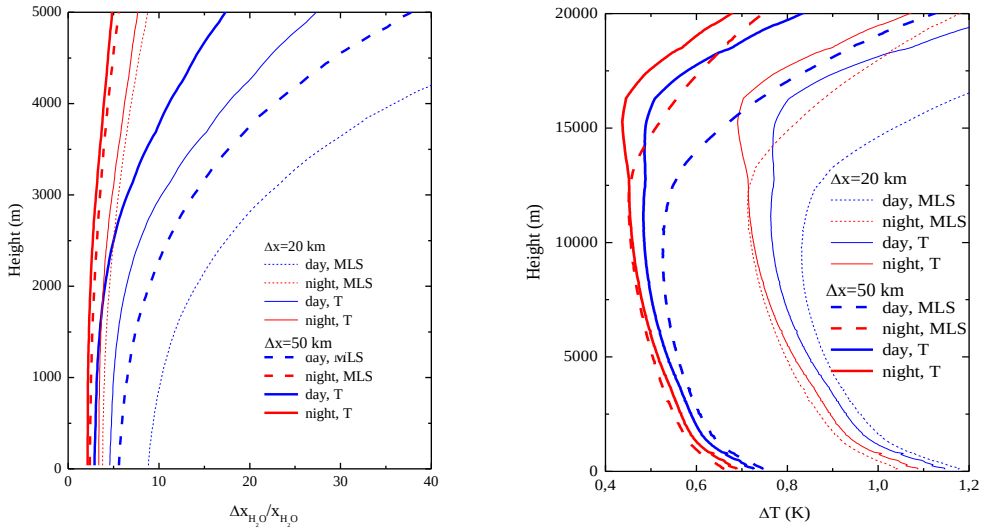

Figure 1. Vertical profiles of $\Delta x_{H_2O}(z)/x_{H_2O}(z)$ (panel a) and ΔT (panel b) for the tropical (continuous lines) and mid-latitude summer (dashed lines) reference models. Red lines represent night-time conditions, while blue lines represent daytime conditions. Thin lines represent a horizontal resolution of 20 km, while bold lines represent a horizontal resolution of 50 km.

REFERENCES

[1] Intergovernmental Panel on Climate Change: "Climate Change 2013: The physical science basis," in *5th Assessment Report, IPCC WGI AR5*, edited by T. F. Stocker, D. Qin, G.-K. Plattner, M. Tignor, S. K. Allen, J. Boschung, A. Nauels, Y. Xia, V. Bex and P.M. Midgley (Cambridge University, 2013) Cambridge, U. K.

[2] Intergovernmental Panel on Climate Change: "Climate Change 2014: Impacts, adaptation, and vulnerability," in *5th Assessment Report, IPCC WGII AR5, Technical Summary*, Coordinating Lead Authors: C. Field, V. Barros, K. Mach, and M. Mastrandrea, available at http://www.ipcc.ch/report/ar5/wg2 (IPCC, 2014), Geneva, Switzerland.

[3] Intergovernmental Panel on Climate Change: "Climate Change 2014: Synthesis Report" in *5th Assessment Report, Working Groups I, II and III*, Core Writing Team, R.K. Pachauri and L.A. Meyer (eds.) (IPCC, 2014) Geneva, Switzerland, 151 pp.

[4] D. P. Dee, S. M. Uppala, A. J. Simmons, P. Berrisford, P. Poli, S. Kobayashi, U. Andrae, M. A. Balmaseda, G. Balsamo, P. Bauer, P. Bechtold, A. C. M. Beljaars, L. van de Berg, J. Bidlot, N. Bormann, C. Delsol, R. Dragani, M. Fuentes, A. J. Geer, L. Haimberger, S. B. Healy, H. Hersbach, E. V. Hólm, L. Isaksen, P. Kållberg, M. Köhler, M. Matricardi, A. P. McNally, B. M. Monge-Sanz, J.-J. Morcrette, B.-K. Park, C. Peubey, P. de Rosnay, C. Tavolato, J.-N. Thépaut and F. Vitart, "The ERA-Interim reanalysis: Configuration and performance of the data assimilation system," Q. J. R. Meteorol. Soc. 137, 553–597 (2011).

[5] N. A. Crook, "Sensitivity of moist convection forced by boundary layer processes to low-level thermodynamic fields," Mon. Weather Rev. 124, 1767–1785 (1996).

[6] S. Dierer, M. Arpagaus, A. Seifert, E. Avgoustoglou, R. Dumitrache, F. Grazzini, P. Mercogliano, M. Milelli and K. Starosta, "Deficiencies in quantitative precipitation forecasts: sensitivity studies using the COSMO model," Meteorol. Z. 18, 631–645 (2009).

[7] L. Bengtsson, K. I. Hodges and S. Hagemann, "Sensitivity of the ERA40 reanalysis to the observing system: determination of the global atmospheric circulation from reduced observations," Tellus A 56, 456–471 (2004).

[8] K. Warrach-Sagi, T. Schwitalla, V. Wulfmeyer and H.-S. Bauer, "Evaluation of a climate simulation based on the WRF-NOAH model system: precipitation in Germany," Clim. Dynam. 41, 755–774 (2013).

[9] S. Kotlarski, K. Keuler, O. B. Christensen, A. Colette, M. Déqué, A. Gobiet, K. Goergen, D. Jacob, D. Lüthi, E. van Meijgaard, G. Nikulin, C. Schär, C. Teichmann, R. Vautard, K. Warrach-Sagi and V. Wulfmeyer,

"Regional climate modeling on European scales: a joint standard evaluation of the EURO-CORDEX RCM ensemble," Geosci. Model Dev. 7, 1297–1333 (2014).

[10] V. Wulfmeyer, R. M. Hardesty, D. D. Turner, A. Behrendt, M. P. Cadeddu, P. Di Girolamo, P. Schlüssel, J. Van Baelen and F. Zus, "A review of the remote sensing of lower-tropospheric thermodynamic profiles and its indispensable role for the understanding and the simulation of water and energy cycles," Rev. Geophys. 53, 819–895 (2015).

[11] Lindsay J. Bennett, Alan M. Blyth, Ralph R. Burton, Alan M. Gadian, Tammy M. Weckwerth, Andreas Behrendt, Paolo Di Girolamo, Manfred Dorninger, Sarah-Jane Lock, Victoria H. Smith, Stephen D. Mobs, "Initiation of convection over the Black Forest mountains during COPS IOP15a," Q. J. R. Meteorol. Soc. 137, 176-189 (2011).

[12] World Meteorological Organisation (WMO), Expert Team, Commission on Basic Systems, Working Group on Satellites, Third session, Final Report, No. 1 (World Meteorological Organization, 1998), p. 73.

[13] CEOS, WMO On-line Database, Version 2.5, Observational requirements, http://altostratus.wmo.ch/sat/stations/_asp_htx_idc/Requirements.asp (World Meteorological Organization, 2003).

[14] https://www.wmo-sat.info/oscar for water vapor and temperature

[15] GCOS 2016 Implementation Plan, WMO GCOS-200 (GOOS-214), https://ane4bf-datap1.s3-eu-west-1.amazonaws.com/wmocms/s3fs-public/programme/brochure/GCOS-200_OnlineVersion.pdf?PlowENiCc1RGh9ReoeAoGBT0QhnJYm6_ (World Meteorological Organization, 2016).

[16] P. Di Girolamo, A. Behrendt and V. Wulfmeyer, "Spaceborne profiling of atmospheric temperature and particle extinction with pure rotational Raman Lidar and of relative humidity in combination with differential absorption Lidar: performance simulations," Appl. Opt. 45, 2474-2494 (2006).

[17] P. Di Girolamo, A. Behrendt and V. Wulfmeyer, "Space-borne profiling of atmospheric thermodynamic variables with Raman lidar: Performance simulations, Opt. Express, 26(7), 8165-8161(2018).

[18] N. D. Whiteman, , S. H. Melfi,, and R. A. Ferrare, "Raman lidar system for measurement of water vapor and aerosols in the Earth's atmosphere," Appl. Opt. 31**,** 3068–3082 (1992).

[19] A. Behrendt and Reichardt, J., "Atmospheric temperature profiling in the presence of clouds with a pure rotational Raman lidar by use of an interference-filter-based polychromator," Appl. Opt. 39, 1372–1378 (2000).

[20] I. Mattis, A. Ansmann, D. Althausen, V. Jaenisch, U. Wandinger, D. Müller, Y. F. Arshinov, S. M. Bobrovnikov and I. B. Serikov, "Relative-humidity profiling in the troposphere with a Raman lidar," Appl. Opt. 41, 6451-6462 (2002).

[21] A. Behrendt, T. Nakamura, M. Onishi, R. Baumgart and T. Tsuda, "Combined Raman lidar for the measurement of atmospheric temperature, water vapor, particle extinction coefficient, and particle backscatter coefficient," Appl. Opt. 41, 7657–7666 (2002).

[22] A. Behrendt, T. Nakamura and T. Tsuda, "Combined temperature lidar for measurements in the troposphere, stratosphere, and mesosphere," Appl. Opt. 43, 2930-2939 (2004).

[23] A. Behrendt, V. Wulfmeyer, E. Hammann, S. K. Muppa and S. Pal, "Profiles of second to third order moments of turbulent temperature fluctuations in the convective boundary layer: First measurements with rotational Raman lidar", Atmos. Chem. Phys. 15, 5485-5500 (2015).

[24] P. Di Girolamo, R. Marchese, D. N. Whiteman and B. B. Demoz, "Rotational Raman Lidar measurements of atmospheric temperature in the UV," Geophys. Res. Lett. 31, L01106 (2004).

[25] P. Di Girolamo, A. Behrendt, C. Kiemle, V. Wulfmeyer, H. Bauer, D. Summa, A. Dörnbrack and G. Ehret, "Simulation of satellite water vapour lidar measurements: Performance assessment under real atmospheric conditions," Remote Sens. Environ. 112, 1552-1568 (2008).

[26] P. Di Girolamo, D. Summa, R. Ferretti, "Multiparameter Raman Lidar Measurements for the Characterization of a Dry Stratospheric Intrusion Event," J. Atmos. Ocean. Tech. 26, 1742-1762 (2009).

[27] M. Radlach, A. Behrendt and V. Wulfmeyer, "Scanning rotational Raman lidar at 355 nm for the measurement of tropospheric temperature fields," Atmos. Chem. Phys. 8, 159–169 (2008).

[28] Turner, D. D., and J. E. M. Goldsmith, "Twenty-four-hour Raman lidar water vapor measurements during the Atmospheric Radiation Measurement Program's 1996 and 1997 water vapor intensive observation periods," J. Atmos. Oceanic Technol., 16, 1062–1076 (1999).

[29] J. Reichardt, U. Wandinger, V. Klein, I. Mattis, B. Hilber and R. Begbie, "RAMSES: "German Meteorological Service autonomous Raman lidar for water vapor, temperature, aerosol, and cloud measurements," Appl. Opt., 51**,** 8111–8131 (2012).
[30] T. Dinoev, V. Simeonov, Y. Arshinov, S. Bobrovnikov, P. Ristori, B. Calpini, M. Parlange and H. van den Bergh, "Raman Lidar for Meteorological Observations, RALMO – Part 1: Instrument description," Atmos. Meas. Tech. 6, 1329-1346 (2013).
[31] E. Hammann and A. Behrendt, "Parametrization of optimum filter passbands for rotational Raman temperature measurements," Opt. Express 23, 30767-30782 (2015).
[32] D. N. Whiteman, R. Kurt and R. Scott, "Airborne and Ground-Based Measurements Using a High-Performance Raman Lidar", J. Atmos. Ocean. Technol. 27(11), 1781–1801 (2010).
[33] B. Liu, Z. Wang, Y. Cai, P. Wechsler, W. Kuestner, M. Burkhart and W. Welch, "Compact airborne Raman lidar for profiling aerosol, water vapor and clouds," Opt. Express 22, 20613-20621 (2014).
[34] W. Decheng, Z. Wang, P. Wechsler, N. Mahon, M. Deng, B. Glover, M. Burkhart, W. Kuestner and B. Heesen, "Airborne compact rotational Raman lidar for temperature measurement," Opt. Express 24, A1210-A1223 (2016).
[35] É. Gérard, D. G. H. Tan, L. Garand, V. Wulfmeyer, G. Ehret, and P. Di Girolamo, "Major advances foreseen in humidity profiling from the Water Vapour Lidar Experiment in Space (WALES)," Bull. Am. Meteorol. Soc. **85**(2), 237–252 (2004).
[36] V. Wulfmeyer, H. Bauer, P. Di Girolamo, and C. Serio, "Comparison of active and passive water vapour remote sensing from space: An analysis based on the simulated performance of IASI and space borne differential absorption Lidar," Remote Sens. Environ. **95**(2), 211–230 (2005).
[37] C. Serio, G. Masiello, F. Esposito, P. Di Girolamo, T. Di Iorio, L. Palchetti, G. Bianchini, G. Muscari, G. Pavese, R. Rizzi, B. Carli, V. Cuomo, "Retrieval of foreign-broadened water vapor continuum coefficients from emitted spectral radiance in the H2O rotational band from 240 to 590 cm^{-1}. Opt. Express, 16(20), 15816-15833, (2008).
[38] D. N. Whiteman, S. H. Melfi and R. A. Ferrare, "Raman lidar system for the measurement of water vapor and aerosols in the Earth's atmosphere," Appl. Opt. 31, 3068–3082 (1992).